Heliyon 10 (2024) e26393

Contents lists available at ScienceDirect

Heliyon

journal homepage: www.cell.com/heliyon

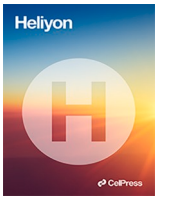

Research article

Disrupted nuclear import of cell cycle proteins in Huntington's/PolyQ disease causes neurodevelopment defects in cellular and Drosophila model

Sandeep Kumar Dubey [a,1], Thomas E. Lloyd [b,c,**], Madhu G. Tapadia [a,*,2]

[a] Cytogenetics Laboratory, Department of Zoology, Banaras Hindu University, Varanasi, Uttar Pradesh, India
[b] Department of Neurology, Johns Hopkins University School of Medicine, Baltimore, MD, USA
[c] The Solomon H. Snyder Department of Neuroscience, Johns Hopkins University School of Medicine, Baltimore, MD, USA

ARTICLE INFO

Keywords:
Drosophila
PolyQ
Huntington's disease
Brain
Nuclear pore complex
Neurodevelopment
CAD neuron
Nucleocytoplasmic transport

ABSTRACT

Huntington's disease is caused by an expansion of CAG repeats in exon 1 of the huntingtin gene encoding an extended PolyQ tract within the Huntingtin protein (mHtt). This expansion results in selective degeneration of striatal medium spiny projection neurons in the basal ganglia. The mutation causes abnormalities during neurodevelopment in human and mouse models. Here, we report that mHtt/PolyQ aggregates inhibit the cell cycle in the Drosophila brain during development. PolyQ aggregates disrupt the nuclear pore complexes of the cells preventing the translocation of cell cycle proteins such as Cyclin E, E2F and PCNA from cytoplasm to the nucleus, thus affecting cell cycle progression. PolyQ aggregates also disrupt the nuclear pore complex and nuclear import in mHtt expressing mammalian CAD neurons. PolyQ toxicity and cell cycle defects can be restored by enhancing RanGAP-mediated nuclear import, suggesting a potential therapeutic approach for this disease.

1. Introduction

The central nervous system is considered as the major site of PolyQ pathogenesis, with patients suffering from a wide variety of symptoms including movement abnormalities, cognitive impairment, and spectrum of psychiatric disturbances. Earlier studies have shown the presence of varying levels of huntingtin (htt) transcripts throughout the brain, heart, placenta, lung, liver, testes, muscle, kidney, and pancreas [1,2]. This protein is involved in cell signaling, intracellular transport, roles in axonal trafficking, gene regulation, and cell survival [1–5]. Molecular mechanisms that attempt to explain how the expression of abnormal polyglutamine proteins leads to cellular dysfunction include transcriptional dysregulation, mitochondrial dysfunction, inflammation, excitotoxicity and failure of ubiquitin-proteasome system and autophagy [6]. The expansion of CAG repeats in the huntingtin gene disrupts the nucleocytoplasmic transport of proteins and RNAs in iPS-derived neurons and postmortem brain of Huntington's patients [7]. Most of the studies are focused on examining the effect of mutant Huntingtin protein in neuronal cells in adults; however, the effect of toxicity of

* Corresponding author.
** Corresponding author. Department of Neurology, Johns Hopkins University School of Medicine, Baltimore, MD, USA.
E-mail addresses: tlloyd4@jhmi.edu (T.E. Lloyd), madhu@bhu.ac.in (M.G. Tapadia).
[1] Present address: Department of Neurology, Baylor College of Medicine, Houston, Texas, USA.
[2] Lead author.

https://doi.org/10.1016/j.heliyon.2024.e26393
Received 20 November 2023; Received in revised form 15 January 2024; Accepted 12 February 2024
Available online 17 February 2024

mutant Huntingtin in brain development has largely been ignored. Abnormalities in brain development have led to altered neuronal homeostasis and enhanced cellular vulnerability to late life stressors. Penney et al. reported that huntingtin mutations affect striatal neurogenesis at birth [8]. R6/2 transgenic Huntington's disease mice shows decreased hippocampal cell proliferation [9,10]. A recent study has shown that Huntington's disease is in fact a disease of neurodevelopment in humans [11]. However, it is not known how mHTT affects the early development of the brain in humans.

Cell cycle is essential for many key processes that occur in a spatiotemporal manner during development and tissue renewal. Nucleocytoplasmic trafficking of cell cycle proteins determines their abilities to regulate the cell cycle, and their concentration varies dramatically during development as cells differentiate into specific cell fates [12,13]. The shuttling of Cyclin A and Cyclin E between cytoplasm and nucleus is fundamentally important for cell cycle regulation [14]. The Ras-related nuclear protein (Ran) is cardinal for cell cycle events and plays a key role in the nucleocytoplasmic transport of cell cycle proteins [15,16].

The nuclear pore complex (NPC) is composed of multiple copies of nuclear pore proteins (also known as nucleoporins or Nups) and is one of the largest and most complex protein structures in the cells. NPCs are involved in nucleocytoplasmic transport, cell cycle, gene regulation, and other cellular processes [17]. A key function of NPC is to mediate the selective transport of macromolecules between nucleus and cytoplasm, where phenylalanine-glycine (FG)-repeat-containing segments in Nups form a diffusion barrier that blocks the free transport of particles larger than ~5 nm [18–20]. Nuclear transport receptors (NTRs) bind to FG-repeat-containing segments in nucleoporins and cargo for the selective transport of macromolecules [18,20]. Together, NPCs are extremely long-lived protein complexes that show structural abnormalities and decay in post-mitotic neurons in aging [21–24].

In the present study, we examined the effect of mHtt in brain development in Drosophila model. We observed that mHtt/PolyQ repeats impair brain development through inhibition of cell cycle. mHtt/PolyQ disrupts the nuclear pore complex and nuclear import in Drosophila and mouse neuronal cells, thus disrupting the nuclear import of cell cycle regulatory proteins E2F, Cyclin E and PCNA from the cytoplasm to the nucleus. Overexpression of RanGAP in PolyQ-expressing cells rescues mitotic cell number and suppresses PolyQ toxicity. This study indicates that mHtt/PolyQ aggregates impair brain development through the inhibition of cell cycle by

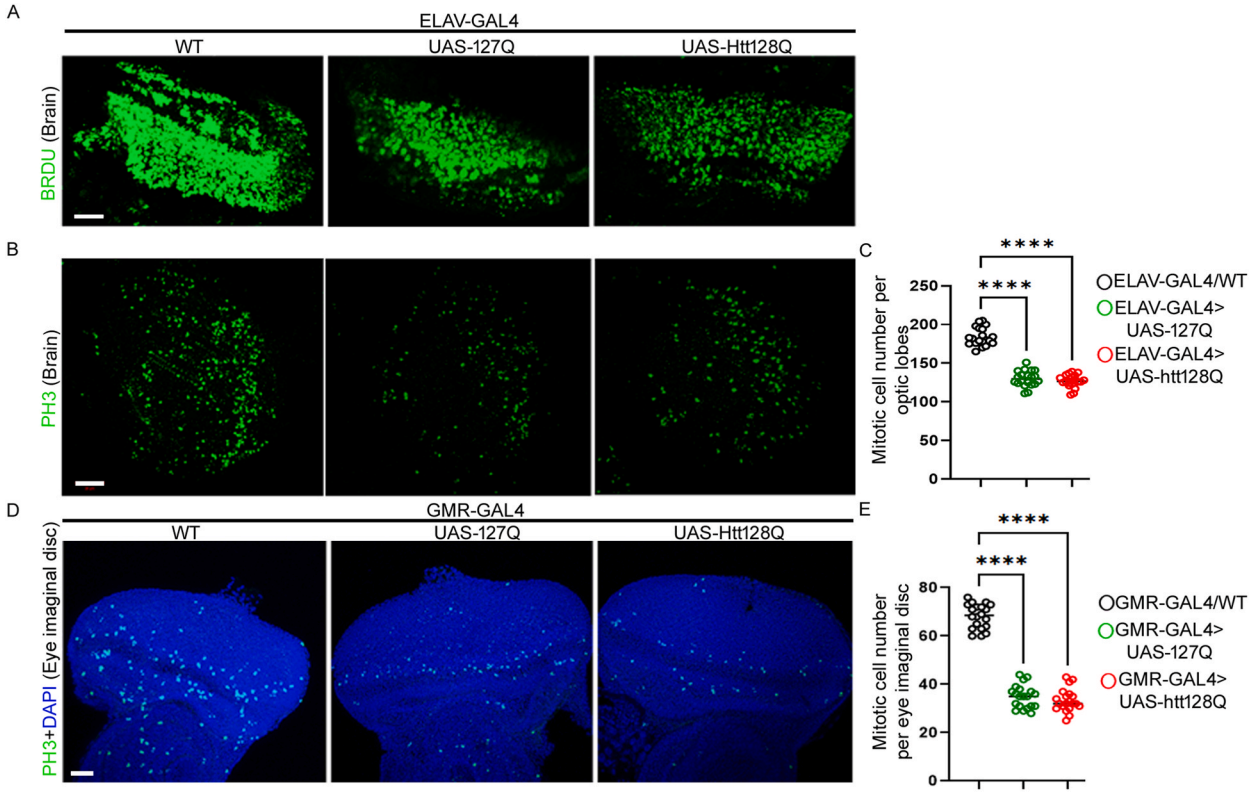

Fig. 1. Overexpression of mHtt/PolyQ repeats inhibit the cell division during development. (A) BrdU (5-bromo-2′-deoxyuridine) staining was done to identify the DNA replicating cells in third instar brain and detected with an anti-BrdU antibody in brain tissue of ELAV-GAL4/WT (control), ELAV-GAL4>UAS-127Q, ELAV-GAL4>UAS-Htt128 genotypes. (Scale bar is 20 μm, n = 20 brains). (B) PH3 staining was done to see the mitotic cell numbers during brain development in ELAV-GAL4/WT (control), ELAV-GAL4>UAS-127Q, ELAV-GAL4>UAS-Htt128 genotypes (Scale bar in a denotes 20 μm). (C) Histogram representing number of DNA replicating (PH3 positive) cells per brain lobe UAS-127Q, UAS-Htt128 using ELAV-GAL4 and control conditions (one-way ANOVA (followed by Tukey's test); n = 20 brain per genotype). (D) PH3 staining (green) was done in eye imaginal discs to see the mitotic cells in mentioned genotypes (Scale bar 50 μm); blue represents DAPI. (E) Histogram showing number of mitotic cells per eye imaginal disc in mentioned genotypes (one-way ANOVA (followed by Tukey's test); n = 20 brain per genotype). (For interpretation of the references to color in this figure legend, the reader is referred to the Web version of this article.)

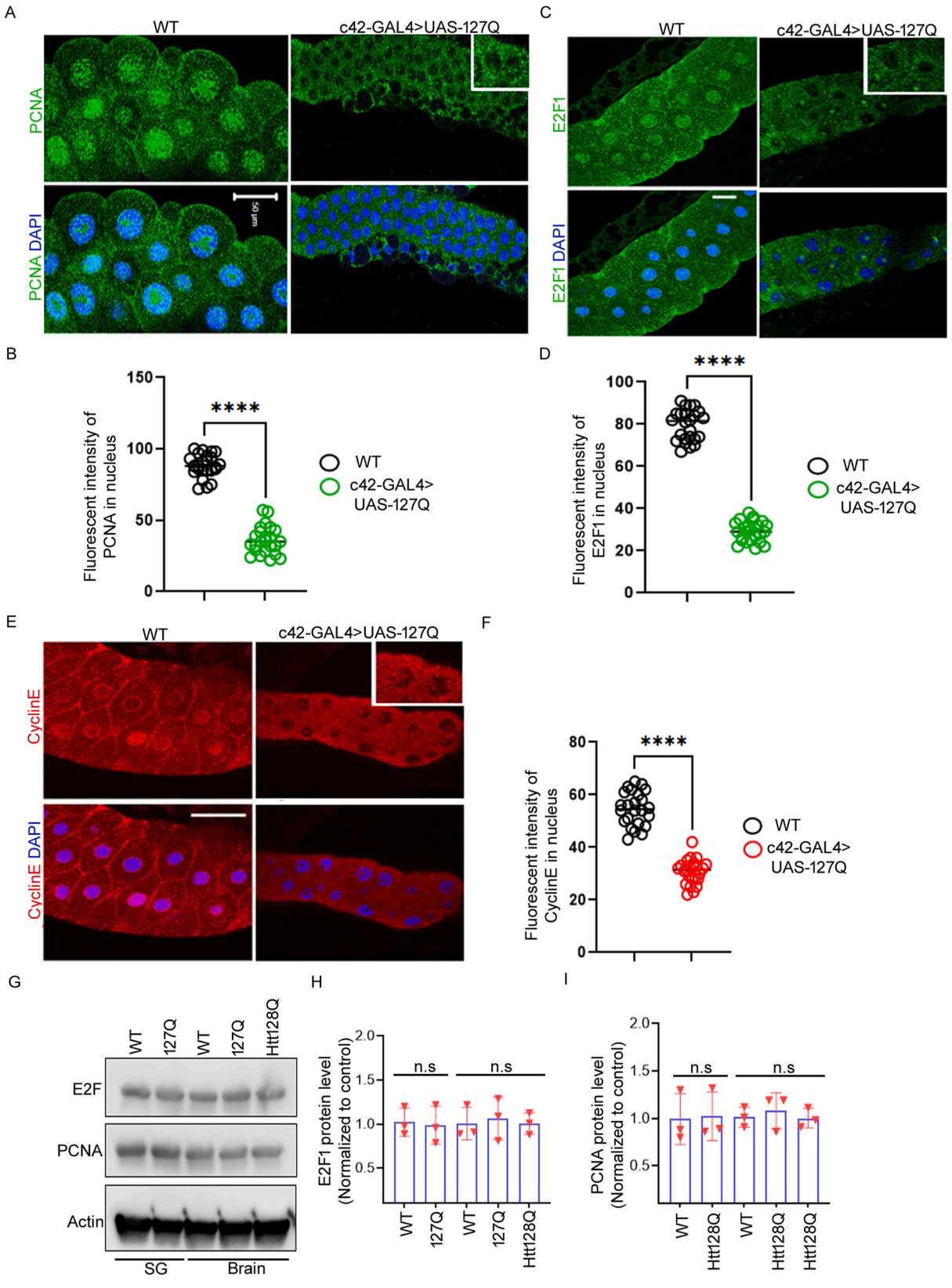

(caption on next page)

Fig. 2. mHtt/PolyQ repeats inhibit nuclear import of cell cycle proteins. (A) Immunofluorescence staining of PCNA (green) with DAPI in following genotypes (c42-GAL4/WT, c42-GAL4>UAS-127Q) in Drosophila larval salivary gland (scale bar denotes 50 μm). (B) Quantification of PCNA immunofluorescence for A, Data are reported as mean ± SEM (mean ± SEM, Unpaired *t*-test; n = 24 cells). (C) Representative confocal image showing E2F1 staining (green) with DAPI of larval salivary gland of genotypes mentioned above of each panel (scale bar: 20 μm). (D) Quantification of E2F1 immunofluorescence in (C), data are reported as mean ± SEM (Unpaired *t*-test, n = 24 cells). (E) Images showing the staining of Cyclin E (Red) with DAPI of salivary glands in mentioned genotypes (Scale bar in image denotes 50 μm). (F) Quantification of Cyclin E fluorescence intensity in (E), data shows mean ± SEM (Unpaired *t*-test; ****P < 0.0001, n = 24 cells). (G) Western blot of E2F1 and PCNA of salivary gland and larval brain of c42-GAL4/WT (control), c42-GAL4 > UAS-127Q and ELAV-GAL4/WT (control), ELAV-GAL4 > UAS-127Q, ELAV-GAL4 > UAS-Htt128 genotypes, respectively. The uncropped and raw blots are shown in Supplementary Fig. 4. (H and I) Quantification of E2F1 and PCNA from Western blot in (G). Data are presented as mean ± SEM (One-way ANOVA, Sidak's multiple comparisons are used for analysis, n = 3). (For interpretation of the references to color in this figure legend, the reader is referred to the Web version of this article.)

disrupting nuclear import of cell cycle proteins.

2. Results

2.1. mHtt/PolyQ repeats reduce the mitotic cell number during neurodevelopment

Several studies have reported the alterations in neurogenesis in animal models and patients of various neurodegenerative conditions including Alzheimer's, Parkinson's, and Huntington's diseases [9,10,25–27]. Barnat et al. reported that mutant Huntingtin impairs human neurodevelopment [11]. Here, we use Drosophila models to understand the effect of mutant Huntingtin on neurogenesis. Cell division was measured by incorporation of the thymidine analog, BrdU into newly synthesized DNA during replication in Drosophila larval brains followed by staining with anti-BrdU antibody. To examine the effect of PolyQ aggregates on cell division in the Drosophila brain, PolyQ repeats (UAS-127Q) were expressed using the neuron-specific Elav-Gal4 driver. Furthermore, findings were verified by expressing human exon 1 of the Huntingtin gene harbouring the 128Q repeat expansion (UAS-Htt128Q). Overexpression of PolyQ repeats and Htt128 reduces cell division as compared to the control (ELAV-GAL4/+) driver alone (Fig. 1A). BrdU staining showed ~40% reduction in mitotic cell number with expression of PolyQ repeats and Htt128Q in neurons as compared to control. This was further corroborated using an anti-PH3 antibody against phosphohistone 3 which marks mitosis during the G2 stage (Fig. 1B and C).

PolyQ repeats were also expressed in the eye imaginal disc using GMR-GAL4 driver to observe the effect on cell division. Eye imaginal discs are well-accepted and appropriate for neuronal cell studies, as they are redundant for life. GMR-GAL4 drives the expression of transgenes posterior to morphogenetic furrow in developing eye imaginal discs. We found that overexpression of PolyQ repeats and Htt128Q reduces cell division in eye imaginal disc of third instar larva (Fig. 1D and E). Reduced staining of BRDU and PH3 in brain and eye imaginal discs indicates that PolyQ repeats and Htt128 impaired cell division.

2.2. PolyQ repeats inhibit the cell cycle by disrupting the nuclear import of cell cycle proteins

To further understand the mechanism for reduced DNA replication in the brain following the expression of PolyQ repeats, we selected salivary glands (SGs) of Drosophila for further experiments, as they have large cell size and follow a highly regulated pattern of endo-replication cycles [28]. Polytene results in increased DNA content and polyploidy. Expression of expanded PolyQ repeats in salivary glands resulted in a marked reduction in the size of glands. The reduction of SGs could be due to two non-mutually exclusive causes, reduced cell number or reduced cell size. We first counted the number of SG cells stained with DAPI and found no statistical difference in the number of cells between SGs expressing PolyQ and wild type (Fig. S1A and S1B). Next, the size of the cells and nuclei were measured, and the size of nucleus was significantly reduced in comparison to wild-type (Fig. S1A–S1E). The reduction in the size of the nucleus was also significant as compared to repeat size of 20Q (Fig. S1C). We measured the DNA content by DAPI staining and it was found to be reduced in SGs expressing PolyQ repeats as compared to wild type (Fig. S1D). These results suggest that PolyQ aggregates could be affecting DNA replication. The size of the cells increases with each round of endoreplication, with the largest cells having undergone the most rounds of replication [29]. This relationship between cell size and the number of rounds of endoreplication is highly regulated.

We next looked at the protein expression and localization of cell cycle regulatory proteins. The proliferating cell nuclear antigen (PCNA) protein is a key regulator of DNA replication and repair. PCNA processes the DNA polymerase δ in eukaryotic cells and is involved in chromatin reorganization, DNA repair, sister-chromatid cohesion, and cell cycle regulation. PCNA was found to be localized in the nucleus as well as cytoplasm in wild type SGs, however in SGs expressing PolyQ repeats, PCNA was present only in the cytoplasm (Fig. 2A and B). Next, we examined the localization of E2F1, which is a critical transcription factor for the cell cycle and is required for Cyclin E expression at the G1-S phase transition [30]. Similar to PCNA, E2F1 was localized in the nucleus as well as cytoplasm in wild-type SGs, whereas overexpression of expanded PolyQ repeats restricts E2F1 to the cytoplasm (Fig. 2C and D). In addition, Cyclin E levels were also examined, as it regulates cell cycle progression by translocating to the nucleus and activating Cdk 2 which controls genes for G1-S phase transition. Cyclin E also shows the same distribution pattern as PCNA and E2F in wild-type and in PolyQ repeat-expressing cells; Cyclin E localization to the nucleus is impaired, and it is only present in the cytoplasm (Fig. 2E and F). To check if along with localization, there is a quantitative difference in the levels of these factors, we performed Western blot analysis for E2F and PCNA in the salivary glands and brain. No significant difference in the levels of E2F or PCNA was observed in PolyQ- or

Htt128Q-expressing salivary glands or brains (Fig. 2G–I), suggesting that expanded PolyQ restricts the translocation of cell cycle determinants from the cytoplasm to the nucleus in the salivary gland, rather than affecting their protein level.

2.3. *mHtt/PolyQ repeats disrupt nucleocytoplasmic transport*

The above results suggest that nucleocytoplasmic transport is impaired, and to confirm this hypothesis, we analyzed the localization of a nucleocytoplasmic shuttling reporter NLS-NES-GFP in which GFP is tagged with both a NLS (nuclear localization signal) and NES (nuclear export signal) (Fig. 3A and B). In control SG cells, NLS-NES-GFP localizes to the both nucleus and cytoplasm, whereas in cells expressing PolyQ repeats or Htt128Q localizes predominantly in the cytoplasm confirming that nuclear import of NLS-NES-GFP is inhibited in these cells. This observation was verified under conditions of reduced number of polyQ repeats, UAS-20Q. The pattern was same as control with distribution of the reporter in both cytoplasm and nucleus, suggesting that the mHTT could be responsible for this erroneous distribution of cell cycle factors. We also found mis-localization of NLS-NES-GFP in motor neurons of the ventral nerve cord (VNC) in larval brains expressing PolyQ repeats or Htt128Q (Fig. 3C and D), indicating that the PolyQ repeats and mHtt128Q affects nucleocytoplasmic transport in Drosophila neurons during development. These results show that PolyQ repeats and Htt128Q reduce nuclear import in Drosophila cells in vivo.

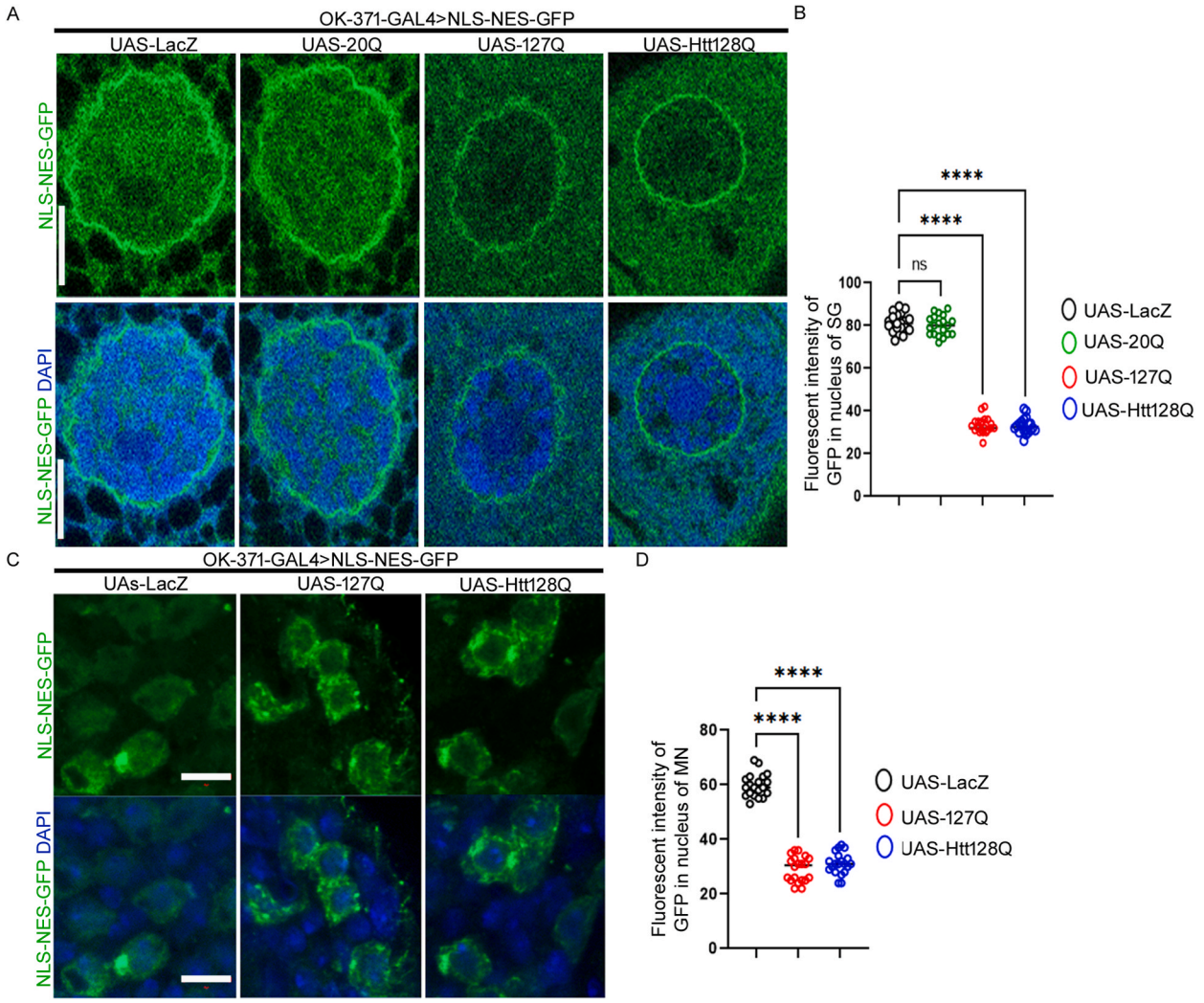

Fig. 3. mHtt/PolyQ repeats inhibit the nuclear imports. (A) NLS-NES-GFP (green) in larval salivary glands of OK371-GAL4/UAS-LacZ (control), OK371-GAL4 > UAS-20Q, OK371-GAL4 > UAS-127Q, and OK371-GAL4 > UAS-Htt128Q genotypes. DAPI (blue) stains the nucleus and scale bar in image denotes 10 μm. (B) Quantification of the nuclear NLS-NES-GFP in salivary gland cell in (A) (One-way ANOVA, Tukey's multiple comparisons test, n = 20 cells). (C) Expression of NLS-NES-GFP (green) in motor neuron of larval ventral nerve card in mentioned genotypes. DAPI (blue) stains the nucleus and scale bar in image denotes 5 μm. (D) Quantification of the nuclear NLS-NES-GFP in motor neuron in (C) (One-way ANOVA, Tukey's multiple comparisons test, n = 20 cells). (For interpretation of the references to color in this figure legend, the reader is referred to the Web version of this article.)

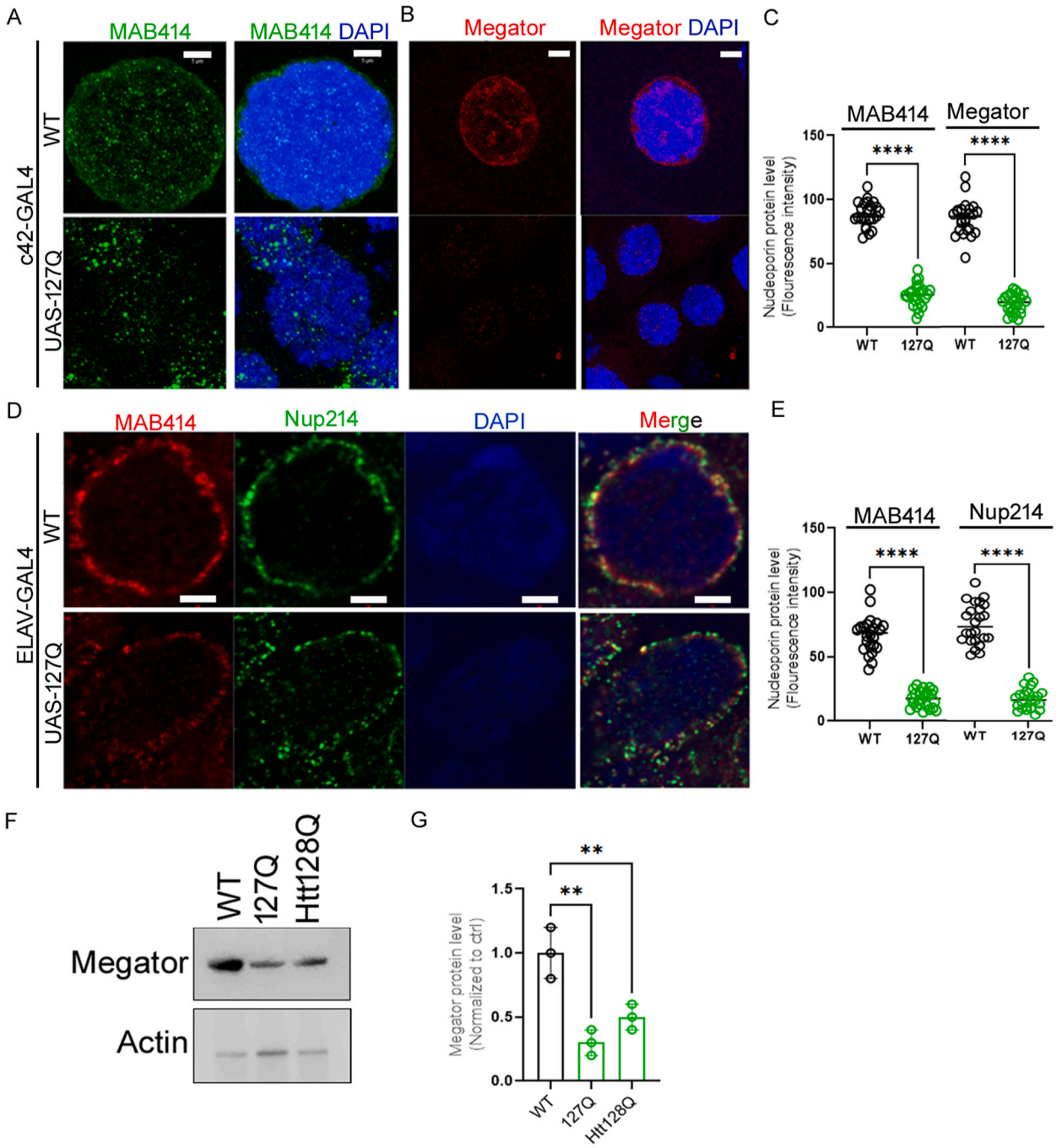

Fig. 4. Nuclear pore complex is disrupted in mHtt/PolyQ repeats expressing cells. (A and B) Larval salivary gland labeled with indicated antibodies recognizing FG-Nucleoporins (MAB414-green) and Megator (red) with DAPI (blue) in following genotypes: c42-GAL4/WT (control), c42-GAL4>UAS-127Q (Scale bar in image denotes 5 μm, n = 24 cells). (C) Quantification of FG-Nucleoporins and Megator in (A) and (B) (Unpaired *t*-test; n = 24 cells). (D) Expansion microscopy image shows MAB414 (Red), Nup214 and DAPI in neuron of ELAV-GAL4/WT and ELAV-GAL4>UAS-127Q (Scale bar is 2 μm). (E) Quantification of FG-Nucleoporins and Nup214 in (D) (Unpaired *t*-test; n = 24 cells). (F) Western blot of salivary gland of c42-GAL4/WT (control), c42-GAL4>UAS-127Q and c42-GAL4>UAS-Htt128Q. The uncropped and raw blots are shown in supplementary Fig. S4. (G) Quantification of Megator from Western blot in (F) (One-way ANOVA (Tukey's multiple comparisons test), n = 20 cells). (For interpretation of the references to color in this figure legend, the reader is referred to the Web version of this article.)

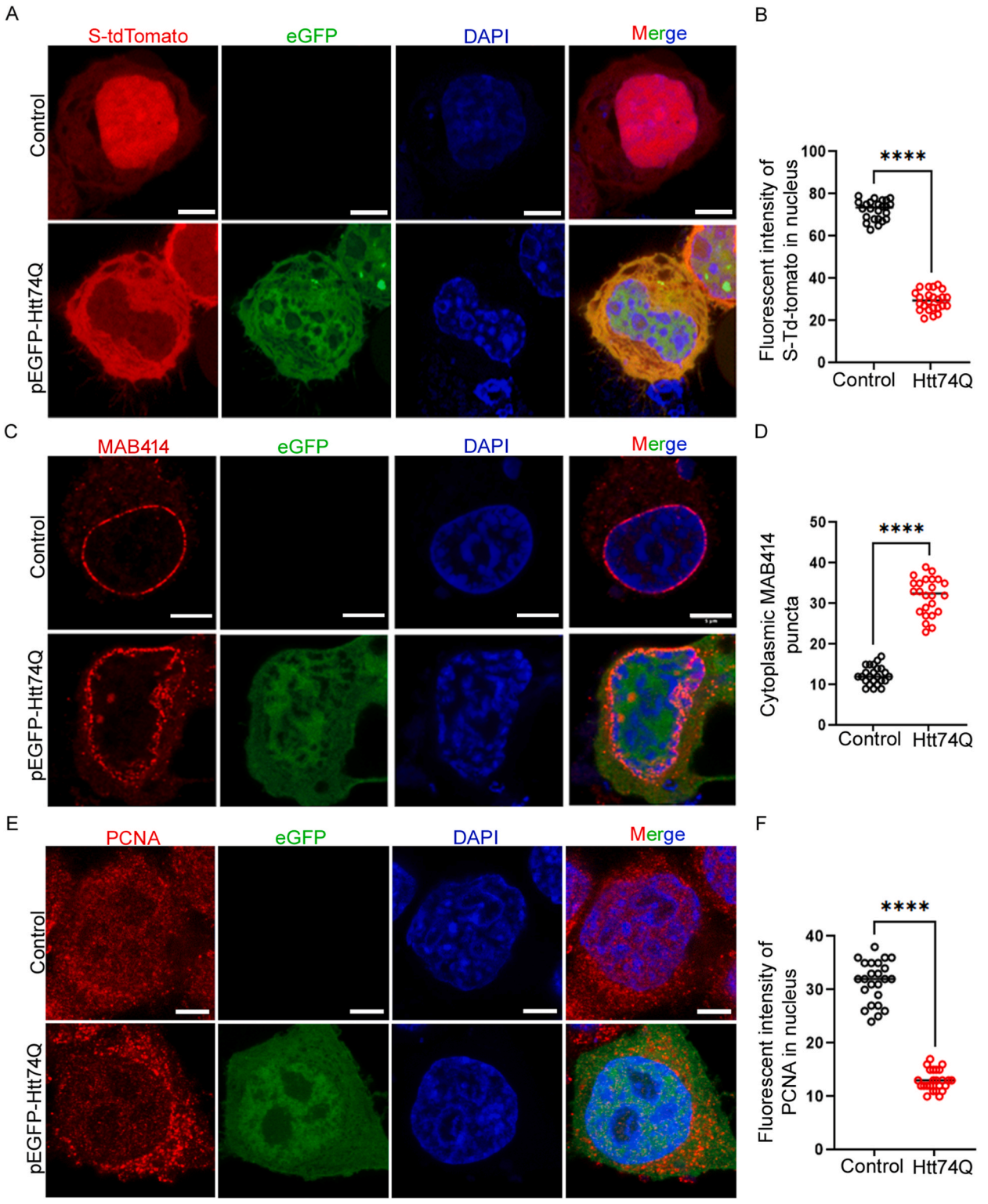

(caption on next page)

Fig. 5. mHtt disrupts the nuclear import and nuclear pore complex in mouse CAD neurons. (A) CAD cells expressing (NLS-NES)S-tdTomato (Red); which shuttles between nucleus and cytoplasm and DAPI (blue) stains the nucleus. pEGFP-Htt74Q (Green) showing the mHtt aggregates in transfected cells, which inhibit the import of S-tdTomato from cytoplasm to nucleus (Scale bar is 2 μm). (B) Quantification of the nuclear S-tdTomato in (A) (Unpaired *t*-test; ****P < 0.0001, n = 24). (C) Optical section of MAB414 (Red) staining showing the nuclear pore complex in CAD neuron. pEGFP-Htt74Q (Green) transfected cells showed the disrupted pattern of nuclear pore complex and mis-localized to cytoplasm. (Scale bar is 2 μm). (D) Quantification of the cytoplasmic puncta of MAB414 in (C) (Unpaired *t*-test; ****P < 0.0001, n = 24). (E) Immunofluorescence staining shows PCNA (red) with mHtt (green) with DAPI (nucleus) in following conditions (scale bar denotes 2 μm). (F) Quantification of PCNA fluorescence intensity of CAD neuronal cells in E, Data shows mean ± SEM (Unpaired *t*-test; n = 24). (For interpretation of the references to color in this figure legend, the reader is referred to the Web version of this article.)

2.4. mHtt/PolyQ repeats disrupt nuclear pore complex integrity in Drosophila

The nuclear membrane is a double membrane lipid bilayer which encloses the nuclear content and allows selective nucleocytoplasmic transport of cellular materials between the cytoplasm and nucleus. The above observation that mHtt/PolyQ repeats affect the nuclear import of cell cycle proteins from the cytoplasm to the nucleus suggested the possibility of defective nuclear pore complexes. We examined the nuclear pore complex (NPC) by immunostaining with Mab414 antibody, which binds to the conserved FG-repeat containing nucleoporins (Nups) within the nuclear pore complex including Nup62, Nup107 and Nup152 and other Nups [31,32].

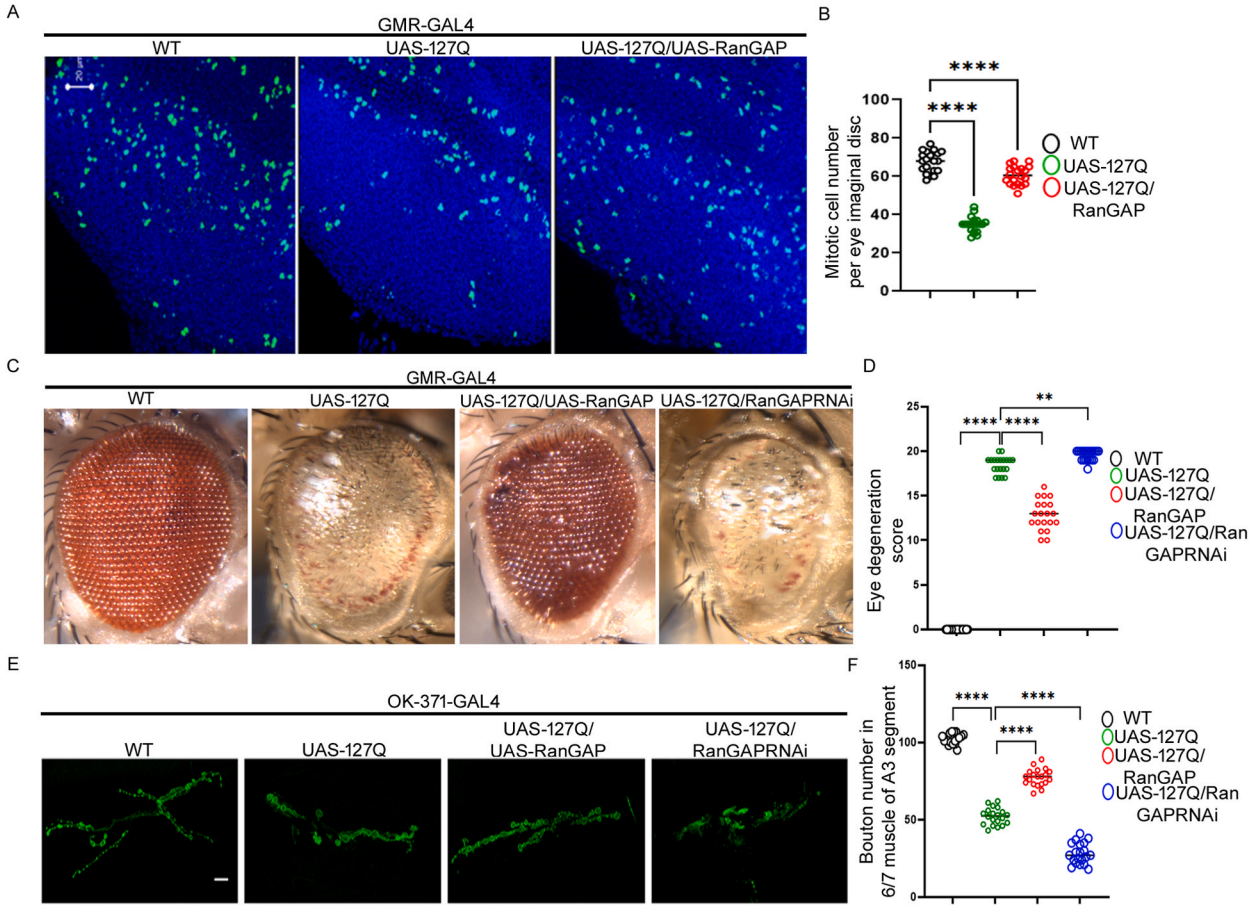

Fig. 6. RanGAP restores the mitotic cell number and suppresses the PolyQ toxicity. (A) PH3 staining (Green) showing the mitotic cell in eye imaginal discs in mentioned genotypes. (Scale bar in image denotes 20 μm). (B) In histogram, PH3-positive cells were counted in per eye imaginal disc in control condition, PolyQ repeats and overexpressing RanGAP in PolyQ repeats background, using GMR-GAL4. (Tukey's multiple comparisons test, n = 20). (C) Photomicrograph images of adult fly eye in GMR-GAL4/WT (control), GMR-GAL4>UAS-127Q, GMR-GAL4>UAS-127Q/UAS-RANGAP and GMR-GAL4>UAS-127Q/UAS-RANGAP-RNAi. (scale bar-100 μm). (D) Quantification of external eye phenotype in (C). Data shows mean ± SEM (One-way ANOVA (Sidak's multiple comparisons), n > 25 adults). (E) The NMJ terminals of the mentioned genotypes immunostained with anti-horseradish peroxidase (HRP) antibody in larvae (OK-371-GAL4/WT, OK-371-GAL4 > UAS-127Q, OK-371-GAL4 > UAS-127Q/UAS-RANGAP and OK371-GAL4 > UAS-127Q/UAS-RANGAP-RNAi). The scale bar is 10 μm. (F) The quantification shows total number of boutons per muscle area on muscle 6/7 of A3 in the above-mentioned genotypes (E) (One-way ANOVA (Sidak's multiple comparisons), n > 25 adults). (For interpretation of the references to color in this figure legend, the reader is referred to the Web version of this article.)

In wild type SGs, NPCs were observed homogeneously distributed on the nuclear membrane (Fig. 4A), while localization of NPCs is nonuniform and reduced in PolyQ expressing-SGs (Fig. 4A and C). We next examined the expression of Megator, as it is also a component of the NPC, and in addition to a role in nucleocytoplasmic transport also plays role in chromosomal organization, mitosis, mRNA transport and gene expression regulation [33,34]. In wild-type nuclei, Megator was present in the form of a rim along the nuclear periphery as well as in the nuclear matrix (Fig. 4B). However, in PolyQ-expressing salivary glands, Megator expression is significantly reduced, and the rim pattern is completely abolished (Fig. 4B and C). These results suggest that PolyQ aggregates might be disrupting the integrity of nuclear pore complexes in the salivary glands.

To confirm if this disruption is specific to a particular tissue type, we repeated the same experiments in neurons of the larval brain (Fig. 4D and E). Similar to our observations in salivary glands, the localization of Nups also appears to be disrupted and reduced in neurons. We also confirmed downregulation of Megator in PolyQ and Htt128Q expressing salivary gland by performing Western blot analysis (Fig. 4F and G), indicating that PolyQ repeats affect the nuclear pore complex in multiple Drosophila cell types.

2.5. mHtt disrupts the nuclear pore complex in mouse CAD neuronal cells

To determine whether findings observed in Drosophila models of Huntington's disease also extend to mammalian models, we analyzed nucleocytoplasmic transport in cultured mammalian neurons. Mouse neuroblastoma CAD (Cath. a-differentiated) cells, a cell line with similar morphology to primary neurons, were used to overexpress a mHuntingtin protein containing 74 PolyQ repeats (Htt74Q). We transfected cells with shuttle-tdTomato, which shuttles between nucleus and cytoplasm in the cell. In control cells, shuttle-tdTomato localizes predominantly to the nucleus, whereas in cells expressing Htt74Q-GFP, it localizes primarily to the cytoplasm (Fig. 5A and B). Furthermore, we examined the integrity of nuclear pore complexes in huntingtin (Htt74Q) cells using MAB414 antibody, which recognises FG-repeats in the nucleoporins of NPC. In control cells, the nuclear pore complex localized precisely on the nuclear periphery (Fig. 5C), whereas in PolyQ expressing cells, the NPCs appeared disrupted. In addition, NPCs are localized in the cytoplasm in Htt74Q-expressing CAD neurons (Fig. 5C and D). Interestingly, we also observed that PCNA mislocalizes to the cytoplasm in Htt74Q-expressing CAD neurons, further suggesting that PolyQ repeats inhibit import of PCNA protein (Fig. 5E and F). These data suggest that PolyQ-mediated disruption of the NPC and nuclear import of cell cycle proteins is conserved in fly and mammalian neurons.

2.6. Overexpression of RanGAP in neurons expressing PolyQ repeats rescues mitotic cell number and suppresses PolyQ-mediated toxicity

After confirming the impairment of nucleocytoplasmic transport of cell cycle protein in mHtt/PolyQ repeat-expressing cells, we tested whether enhancing or downregulating nuclear import by RanGAP rescues the mitotic cell number. RanGAP protein is a master regulator of nucleocytoplasmic transport. We observed that overexpression of RanGAP in PolyQ expressing eye imaginal discs rescues the mitotic cell number (Fig. 6A and B), as well as the size of the cells which are the same size as control (Supplementary Fig. 3A). Interestingly, overexpression of RanGAP also rescues the nuclear import of NLS-NES-GFP in PolyQ-expressing cells (Supplementary Figs. 3A and 3B).

Next, we tested the effect of altering RanGAP genetically by expressing it in GMR-Gal4>UAS-127Q progeny and observing the effect in adult eyes. The expression of expanded PolyQ repeats lead to degeneration of eyes with lack of pigmentation, necrotic patches, improper bristles lattice, and defective eyes (Fig. 6C). We observed that overexpression of RanGAP in PolyQ-expressing eyes showed rescue in eye pigmentation and ommatidial arrangement (Fig. 6C and D). To validate these observations, we performed the reverse experiment and downregulated RanGAP resulted in severe eye degeneration (Fig. 6C and D).

Recent reports show that mutant Huntingtin expression causes axonal growth defects and synaptic loss during development in a mouse model [35]. Here, overexpression of PolyQ repeats in motor neurons caused an ~50% reduction of the number of synaptic boutons that form at the neuromuscular junction (Fig. 6E). We further tested for a genetic interaction between PolyQ repeats and RanGAP, and we found that overexpression of RanGAP in PolyQ repeats background rescued the loss of boutons, whereas downregulation of RanGAP showed severe synaptic bouton degeneration as compared to PolyQ repeats condition (Fig. 6E and F). These data suggest the importance of nucleocytoplasmic transport in PolyQ-mediated synaptic toxicity.

3. Discussion

Neurodevelopmental disorder-associated genes such as CDKL5, MECP2, and FMR1, play a role in cell proliferation and differentiation, and their deficiency in neuronal stem cells causes neurodevelopmental disorders [36]. A recent study has reported that mutant Huntingtin alters neural development in humans [11], though the mechanisms by which neurodevelopmental alterations arise in the human CNS remain elusive. The early phase of HD may be looked as a slow progressive alterations in normal neurodevelopment that eventually transforms into a neurodegenerative disorder and reduced neurogenesis, may be a contributor of disease progression. A small fraction of progenitor cells undergo mitosis in HD carrier as compared to control fetuses, which suggests a subpopulation of proliferating cells are affected. The velocities of nuclear movement in G1 and G2 are slow, causing these phases to broaden whereas the G1/S phase transition duration was reduced in HD.

Previous studies have shown that nucleocytoplasmic transport is disrupted in late-onset neurodegenerative diseases like amyotrophic lateral sclerosis (ALS), Frontotemporal dementia (FTD) and Huntington's disease [7,37–41]. Grima et al. found mislocalization, and aggregation nucleoporins and nuclear transport factors in R6/2 mouse model, iPSC-derived neurons HD patient, and postmortem brains [7]. They also found that a subset of nucleoporins colocalize with mHTT aggregates and colocalization increases in

frequency and diameter with disease progression. Another study on Huntington's disease showed that mHTT aggregates sequesters nuclear pore components and disrupts the function of the NPC in a knock-in mouse model, expressing mutant HTT with ~190 CAG repeats, patient iPSC neurons, and postmortem brains [42]. mHTT also disrupts nuclear envelope and causes mis-localization and aggregation of RanGAP1 and Gle1 proteins. These mis-localized nucleoporins and nuclear transport factors colocalize with mutant HTT aggregates in the nucleus, which suggests sequestration of these proteins into mutant HTT aggregates and functional depletion mechanism.

However, it remains unclear if nucleocytoplasmic transport disruption in mHtt/PolyQ repeats per se impact neurodevelopment at early stages of pathogenesis. In this study, we have identified that mHtt/PolyQ repeats alter the molecular and cellular cell cycle program in the Drosophila brain by disrupting the nuclear import of cell cycle proteins during development. In this study, we observed that defects in nucleocytoplasmic transport in mHtt/PolyQ diseases reduce mitotic division in eye imaginal discs and neuro-development in larval stages. Molero et al. reported that development of stem cell-mediated striatal neurogenesis is impaired in Huntington's disease mouse model [43]. In spite of altered transcription and translational levels due to PolyQ aggregates, they do not alter the expression of cell cycle proteins but rather affect their localization. Interestingly, we observed that nuclear import of NLS-NES-GFP is disrupted in neurons of the Drosophila brain. Furthermore, we also found that nuclear import was disrupted in mHtt-expressing mammalian neuronal cell culture, suggesting mHtt/PolyQ repeats inhibit nuclear import of proteins in both cellular and Drosophila models. Using a mammalian neuronal cell model of Huntington's disease, we provide evidence that mHtt disrupts nucleocytoplasmic transport by disrupting the nuclear pore complex. Since mHtt inhibits the nuclear import of cell cycle proteins, it will be interesting to examine whether mHtt also inhibits import of other pathway proteins.

In addition, we have also demonstrated that altering the levels of RanGAP (regulator of nucleocytoplasmic transport) suppresses toxicity in the eye and synaptic loss at the neuromuscular junction. These data suggest that Drosophila and CAD neurons can be used as models to study the mechanism whereby mHtt/PolyQ repeats cause impaired neurodevelopment, since it disrupts the nuclear pore complex and nuclear import of key regulators of cell cycle proteins (Fig. 7). Finally, this work provides evidence linking impairments in nucleocytoplasmic transport with neurodevelopment in Huntington's disease. Our findings suggest that mHtt/PolyQ aggregates affect the cell cycle by disrupting the nuclear import machinery, thereby leading to abnormalities in neurodevelopment.

4. Materials and methods

4.1. Fly stocks and culture conditions

Flies were normally maintained on standard Drosophila agar cornmeal medium at 25 °C. The following stocks were procured from Bloomington drosophila Stock Center until mentioned: c42-GAL4 (BDSC-30835), GMR-GAL4 (BDSC-9146) UAS-127Q [44]. Bloominton stocks: Oregon R^{+} was used as WT control. UAS-RanGAP (BDSC-22503 and 16995), RanGAP-RNAi (BDSC-29565), OK-371-GAL4 (BDSC- 26160), UAS-NLS-NES-GFP [41], ELAV-GAL4 (BDSC-8765), UAS-Htt128Q (Littleton's Lab, MIT).

Eye degeneration was scored based on the work by J Paul Taylor [45,46]. The eye degeneration phenotype was quantified based on the following criteria: Drosophila eyes were looked for the changes in supernumerary inter-ommatidial bristles with disrupted

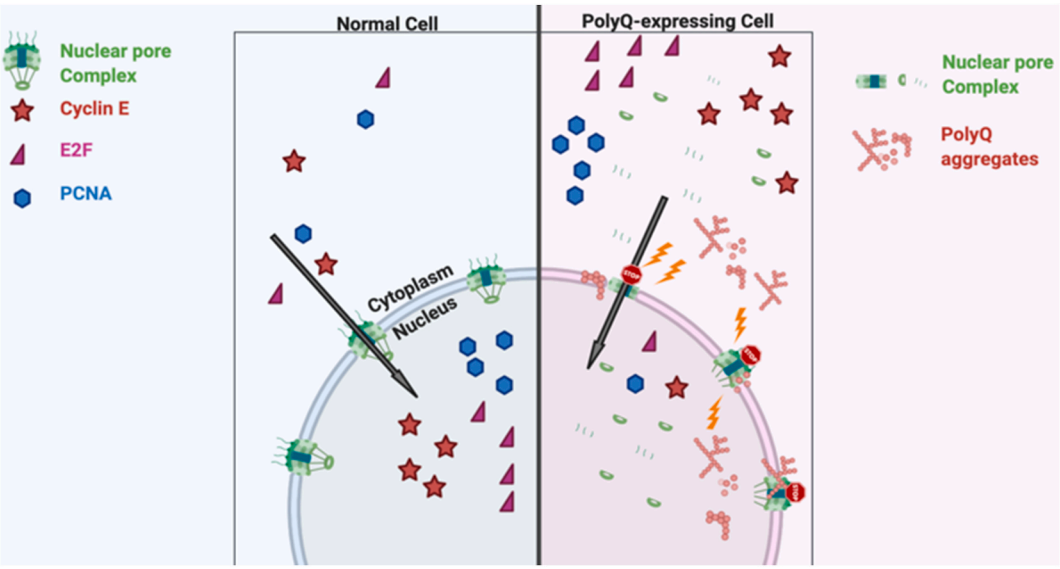

Fig. 7. mHtt/PolyQ repeats lead to nuclear import defects and cause neurodevelopment abnormalities. In healthy cells, protein and RNA transport through the nuclear pore complex is an extremely regulated process. In mHtt/PolyQ repeats expressing cell, the structure of nuclear pore complex is compromised, and the transport of proteins and RNAs is no longer controlled. This impairs the import of cell cycle proteins (E2F1, CyclinE and PCNA), further disrupting the cell cycle process.

orientation, black necrotic patches, decrease in eye size, crumbled retina, fused ommatidia, disrupted ommatidial array and lack of pigmentation in adult male flies. Phenotypes were scored for complete loss of inter-ommatidial bristles (+1), if there was more than 3 small or 1 large necrotic black patch in an eye (+1), retinal collapse phenotype expanded to the midline of the eye scored (+1) or beyond (+2). ~50% loss of ommatidia scored (+1) and >50% loss of ommatidia scored (+2). Due to loss of pigmentation resulted change in eye color into orange (+1) or light orange/white (+2) [41,46].

4.2. Immunostaining, antibody, and confocal imaging

Imaginal discs from Drosophila eyes were dissected and fixed with 4% Paraformaldehyde prepared in 1× PBS for about 20 min. These tissues were then washed with PBST (1XPBS, 0.1% Triton X-100). Later, tissues were blocked for 2 h in prepared blocking solution (1× PBS, 0.1% Triton X-100, 0.1% BSA, 10% FCS, and 0.02% Thiomersal). The sample was then incubated with primary antibody at 4 °C overnight. Tissues were then washed with 0.1% PBST (3 × 20 min each) to remove excess antibody and incubated with secondary antibody at room temperature for 2 h. The sample was then stained with DAPI for 10 min, washed thrice with 0.1% PBST and mounted in DABCO (Sigma).

The primary antibodies used were obtained from following resources: rabbit anti-HA (1:40, SCBT), Cyclin E (1:50, SCBT), Anti-E2f1 (1:100, gift from Robert J. Duronio), mouse Anti-PCNA (1:300, SCBT), Anti-Megator (1:20, gift from Dr. Harald Saumweber), Anti-NPC antibody [Mab414] (Abcam, USA), guinea pig anti-Nup214 (Prof. Christos Samakovlis, Stockholm), mouse phospho-histone 3 PH3 antibody (1:800, Upstate USA Inc and EMD Millipore), FITC-conjugated anti-HRP (Jackson ImmunoResearch Laboratories) and DAPI (1 mg/ml, Molecular Probe). Imaging was done using Zeiss LSM 510 and 800 Meta Confocal microscopes. Adobe Photoshop was used for processing and image assembly. Zen Zeiss software was used for quantification of fluorescence intensities. The individual values are the mean value of fluorescence intensity of the protein of area of individual cell or region.

4.3. BrdU staining

Grace's insect medium was used to dissect the brains from 3rd instar larvae. These larvae were then incubated with 200 μg/ml BrdU for half an hour. The sample was then fixed using 4% paraformaldehyde for 30 min and subsequently treated with 2 N HCl for 20 min. Anti-BrdU antibody (ab6326) (1:10 dilution) was used to detect the BrDU incorporation in the larval brain followed by incubation of sample with secondary antibody diluted 1:500 in blocking solution.

4.3.1. Expansion microscopy

Brains were processed for Expansion Microscopy after immunostaining, according to the protocol mentioned in Dubey et al., 2022 [41,47]. Immunostained brains were washed in 0.1% PBST before proceeding with steps for anchoring proteins to sample buffer with 0.1 mg/ml Acryloyl-X SE (AcX) in PBS for 12 h. The samples were then taken for gelation by adding gelling solution incubating them on ice for 2 h before pipetting the brains onto the Gel Chamber composed of a glass slide, spacers, and a cover glass. The Gel Chamber was then incubated at 37 °C for ~1 h. Embedded brains were then trimmed from the gel chamber upon gel solidification and submerged in the Digestion Buffer with fresh Proteinase K (1:100) for 12 h. The brains were washed with ddH_2O several times to remove excess proteinase K. The samples were then mounted on the slide with dH2O and imaged on Zeiss LSM800 with 63× Objective.

4.4. Western blot

The protein samples were prepared from the larval brain and salivary gland (112–120 h) of the desired genotype. The brain and salivary glands were dissected in 1× PBS and were transferred and crushed in RIPA buffer for protein extraction. Samples were denatured at 95 °C for 10 min, followed by centrifugation at 12000 rpm for 10 min to remove debris. Supernatant was collected and subjected to SDS-PAGE gel. Protein was then transferred onto a PVDF membrane from SDS-PAGE gel using wet electrotransfer at 100 V for 2 h in the cold room. The PVDF membrane was incubated in the blocking solution (5% milk in PBST) for 2 h followed by 1° antibody incubation (antibody in 2% blocking solution) for 12 h at 4 °C. The membrane was washed in 1× TBST (3 times, in 15 min each) and was incubated in secondary antibody for 2 h at room temperature followed by 3× PBST washes. Enhanced chemiluminescence (ECL) method was used to detect the signal on LI-COR Biosciences.

4.5. Cell culture and plasmids

CAD (Cath.-a-differentiated) cells were received from Zhou lab, JHMI and CAD cells were cultured in DMEM/F12 (1:1, Thermo Fisher (Gibco)) supplemented with 10% FBS and 1× Penicillin-Streptomycin Solution in a standard humidified 5% CO_2, 37 °C cell culture incubator. The CAD cells were transfected with S-tdTomato [44] and htt74Q-EGFP (Addgene) using Lipofectamine (Thermo Fisher) and Opti-MEM (Thermo Fisher) at 80% confluency.

4.6. Statistical analyses

All Statistical analysis was done with Prism software. All experiments were performed in triplicate and the data showed as mean ± standard deviation (SD) from at least 3 independent experiments. The P values less than 0.05 were considered statistically significant.

Data and code availability

All data reported in this article will be available from the lead contact upon request.
This paper does not report any original code.

CRediT authorship contribution statement

Sandeep Kumar Dubey: Writing – review & editing, Writing – original draft, Visualization, Validation, Resources, Formal analysis, Data curation, Conceptualization. **Thomas E. Lloyd:** Writing – review & editing, Writing – original draft, Supervision, Resources, Project administration, Investigation. **Madhu G. Tapadia:** Writing – review & editing, Writing – original draft, Supervision, Resources, Project administration, Investigation, Funding acquisition, Formal analysis.

Declaration of competing interest

Madhu G Tapadia and Thomas E Lloyd reports financial support was provided by Department of Science and Technology (DST), New Delhi, Department of Biotechnology (DBT), New Delhi. NIH grants R01NS094239 and R01AG068043 and the Packard Center for ALS Research at Johns Hopkins School of Medicine. Madhu G Tapadia reports a relationship with Department of Science and Technology (DST), New Delhi and Department of Biotechnology (DBT) New Delhi that includes: funding grants. Thomas E Lloyd reports a relationship with NIH grants R01NS094239 and R01AG068043 and the Packard Center for ALS Research at Johns Hopkins School of Medicine that includes: funding grants. If there are other authors, they declare that they have no known competing financial interests or personal relationships that could have appeared to influence the work reported in this paper.

Acknowledgments

We thank Parsa Kazemi-Esfarjani (Caltech), Littleton's Lab (MIT) and Bloomington Drosophila stock Centre (BDSC) for transgenic flies. This work was supported by research grant from Department of Science and Technology (DST), New Delhi and Department of Biotechnology (DBT) Government of India, New Delhi. We thank the DST India and Johns Hopkins Multiphoton Imaging Core facility (NS050274) for Confocal Microscope. This work was also supported by NIH grants R01NS094239 and R01AG068043 and the Packard Center for ALS Research at Johns Hopkins School of Medicine.

Appendix A. Supplementary data

Supplementary data to this article can be found online at https://doi.org/10.1016/j.heliyon.2024.e26393.

References

[1] S.H. Li, G. Schilling, W.S. Young 3rd, X.J. Li, R.L. Margolis, O.C. Stine, M.V. Wagster, M.H. Abbott, M.L. Franz, N.G. Ranen, et al., Huntington's disease gene (IT15) is widely expressed in human and rat tissues, Neuron 11 (5) (1993) 985–993, https://doi.org/10.1016/0896-6273(93)90127-d.
[2] T.V. Strong, D.A. Tagle, J.M. Valdes, L.W. Elmer, K. Boehm, M. Swaroop, K.W. Kaatz, F.S. Collins, R.L. Albin, Widespread expression of the human and rat Huntington's disease gene in brain and nonneural tissues, Nat. Genet. 5 (3) (1993) 259–265, https://doi.org/10.1038/ng1193-259.
[3] Y. Trottier, D. Devys, G. Imbert, F. Saudou, I. An, Y. Lutz, C. Weber, Y. Agid, E.C. Hirsch, J.L. Mandel, Cellular localization of the Huntington's disease protein and discrimination of the normal and mutated form, Nat. Genet. 10 (1) (1995) 104–110, https://doi.org/10.1038/ng0595-104.
[4] A.H. Sharp, S.J. Loev, G. Schilling, S.H. Li, X.J. Li, J. Bao, M.V. Wagster, J.A. Kotzuk, J.P. Steiner, A. Lo, et al., Widespread expression of Huntington's disease gene (IT15) protein product, Neuron 14 (5) (1995) 1065–1074, https://doi.org/10.1016/0896-6273(95)90345-3.
[5] J. Schulte, J.T. Littleton, The biological function of the Huntingtin protein and its relevance to Huntington's Disease pathology, Curr. Trends Neurol. 5 (2011) 65–78.
[6] C. Landles, G.P. Bates, Huntingtin and the molecular pathogenesis of Huntington's disease. Fourth in molecular medicine review series, EMBO Rep. 5 (10) (2004) 958–963, https://doi.org/10.1038/sj.embor.7400250.
[7] J.C. Grima, J.G. Daigle, N. Arbez, K.C. Cunningham, K. Zhang, J. Ochaba, C. Geater, E. Morozko, J. Stocksdale, J.C. Glatzer, J.T. Pham, I. Ahmed, Q. Peng, H. Wadhwa, O. Pletnikova, J.C. Troncoso, W. Duan, S.H. Snyder, L.P.W. Ranum, L.M. Thompson, T.E. Lloyd, C.A. Ross, J.D. Rothstein, Mutant huntingtin disrupts the nuclear pore complex, Neuron 94 (1) (2017), https://doi.org/10.1016/j.neuron.2017.03.023, 93-107.e106.
[8] J.B. Penney Jr., J.P. Vonsattel, M.E. MacDonald, J.F. Gusella, R.H. Myers, CAG repeat number governs the development rate of pathology in Huntington's disease, Ann. Neurol. 41 (5) (1997) 689–692, https://doi.org/10.1002/ana.410410521.
[9] S.E. Lazic, H. Grote, R.J. Armstrong, C. Blakemore, A.J. Hannan, A. van Dellen, R.A. Barker, Decreased hippocampal cell proliferation in R6/1 Huntington's mice, Neuroreport 15 (5) (2004) 811–813, https://doi.org/10.1097/00001756-200404090-00014.
[10] J.M. Gil, P. Mohapel, I.M. Araújo, N. Popovic, J.Y. Li, P. Brundin, A. Petersén, Reduced hippocampal neurogenesis in R6/2 transgenic Huntington's disease mice, Neurobiol. Dis. 20 (3) (2005) 744–751, https://doi.org/10.1016/j.nbd.2005.05.006.
[11] M. Barnat, M. Capizzi, E. Aparicio, S. Boluda, D. Wennagel, R. Kacher, R. Kassem, S. Lenoir, F. Agasse, B.Y. Braz, J.P. Liu, J. Ighil, A. Tessier, S.O. Zeitlin, C. Duyckaerts, M. Dommergues, A. Durr, S. Humbert, Huntington's disease alters human neurodevelopment, Science 369 (6505) (2020) 787–793, https://doi.org/10.1126/science.aax3338.
[12] B.A. Edgar, C.P. Kiehle, G. Schubiger, Cell cycle control by the nucleo-cytoplasmic ratio in early Drosophila development, Cell 44 (2) (1986) 365–372, https://doi.org/10.1016/0092-8674(86)90771-3.
[13] Y. Shindo, A.A. Amodeo, Modeling the role for nuclear import dynamics in the early embryonic cell cycle, Biophys. J. 120 (19) (2021) 4277–4286, https://doi.org/10.1016/j.bpj.2021.05.005.

[14] M. Jackman, Y. Kubota, N. den Elzen, A. Hagting, J. Pines, Cyclin A- and cyclin E-Cdk complexes shuttle between the nucleus and the cytoplasm, Mol. Biol. Cell 13 (3) (2002) 1030–1045, https://doi.org/10.1091/mbc.01-07-0361.

[15] P.R. Clarke, C. Zhang, Spatial and temporal coordination of mitosis by Ran GTPase, Nat. Rev. Mol. Cell Biol. 9 (6) (2008) 464–477, https://doi.org/10.1038/nrm2410.

[16] P. Kaláb, A. Pralle, E.Y. Isacoff, R. Heald, K. Weis, Analysis of a RanGTP-regulated gradient in mitotic somatic cells, Nature 440 (7084) (2006) 697–701, https://doi.org/10.1038/nature04589.

[17] A. Ibarra, M.W. Hetzer, Nuclear pore proteins and the control of genome functions, Gene Dev. 29 (4) (2015) 337–349, https://doi.org/10.1101/gad.256495.114.

[18] D. Mohr, S. Frey, T. Fischer, T. Güttler, D. Görlich, Characterisation of the passive permeability barrier of nuclear pore complexes, EMBO J. 28 (17) (2009) 2541–2553, https://doi.org/10.1038/emboj.2009.200.

[19] M.P. Rout, J.D. Aitchison, A. Suprapto, K. Hjertaas, Y. Zhao, B.T. Chait, The yeast nuclear pore complex: composition, architecture, and transport mechanism, J. Cell Biol. 148 (4) (2000) 635–651, https://doi.org/10.1083/jcb.148.4.635.

[20] K. Ribbeck, D. Görlich, Kinetic analysis of translocation through nuclear pore complexes, EMBO J. 20 (6) (2001) 1320–1330, https://doi.org/10.1093/emboj/20.6.1320.

[21] M.A. D'Angelo, M. Raices, S.H. Panowski, M.W. Hetzer, Age-dependent deterioration of nuclear pore complexes causes a loss of nuclear integrity in postmitotic cells, Cell 136 (2) (2009) 284–295, https://doi.org/10.1016/j.cell.2008.11.037.

[22] M.W. Hetzer, The role of the nuclear pore complex in aging of post-mitotic cells, Aging 2 (2) (2010) 74–75, https://doi.org/10.18632/aging.100125.

[23] J.N. Savas, B.H. Toyama, T. Xu, J.R. Yates 3rd, M.W. Hetzer, Extremely long-lived nuclear pore proteins in the rat brain, Science 335 (6071) (2012) 942, https://doi.org/10.1126/science.1217421.

[24] B.H. Toyama, J.N. Savas, S.K. Park, M.S. Harris, N.T. Ingolia, J.R. Yates 3rd, M.W. Hetzer, Identification of long-lived proteins reveals exceptional stability of essential cellular structures, Cell 154 (5) (2013) 971–982, https://doi.org/10.1016/j.cell.2013.07.037.

[25] N.J. Haughey, A. Nath, S.L. Chan, A.C. Borchard, M.S. Rao, M.P. Mattson, Disruption of neurogenesis by amyloid beta-peptide, and perturbed neural progenitor cell homeostasis, in models of Alzheimer's disease, J. Neurochem. 83 (6) (2002) 1509–1524, https://doi.org/10.1046/j.1471-4159.2002.01267.x.

[26] K. Jin, A.L. Peel, X.O. Mao, L. Xie, B.A. Cottrell, D.C. Henshall, D.A. Greenberg, Increased hippocampal neurogenesis in Alzheimer's disease, Proc. Natl. Acad. Sci. U. S. A. 101 (1) (2004) 343–347, https://doi.org/10.1073/pnas.2634794100.

[27] G.U. Höglinger, P. Rizk, M.P. Muriel, C. Duyckaerts, W.H. Oertel, I. Caille, E.C. Hirsch, Dopamine depletion impairs precursor cell proliferation in Parkinson disease, Nat. Neurosci. 7 (7) (2004) 726–735, https://doi.org/10.1038/nn1265.

[28] Zhimulev, I. F., and D. E. Koryakov. Polytene chromosomes. In Encyclopedia of Life Sciences.

[29] B.A. Edgar, T.L. Orr-Weaver, Endoreplication cell cycles: more for less, Cell 105 (3) (2001) 297–306, https://doi.org/10.1016/s0092-8674(01)00334-8.

[30] D.G. Johnson, J.K. Schwarz, W.D. Cress, J.R. Nevins, Expression of transcription factor E2F1 induces quiescent cells to enter S phase, Nature 365 (6444) (1993) 349–352, https://doi.org/10.1038/365349a0.

[31] M. Fornerod, M. Ohno, M. Yoshida, I.W. Mattaj, CRM1 is an export receptor for leucine-rich nuclear export signals, Cell 90 (6) (1997) 1051–1060, https://doi.org/10.1016/s0092-8674(00)80371-2.

[32] R.W. Wozniak, G. Blobel, The single transmembrane segment of gp210 is sufficient for sorting to the pore membrane domain of the nuclear envelope, J. Cell Biol. 119 (6) (1992) 1441–1449, https://doi.org/10.1083/jcb.119.6.1441.

[33] J.M. Vaquerizas, R. Suyama, J. Kind, K. Miura, N.M. Luscombe, A. Akhtar, Nuclear pore proteins nup153 and megator define transcriptionally active regions in the Drosophila genome, PLoS Genet. 6 (2) (2010) e1000846, https://doi.org/10.1371/journal.pgen.1000846.

[34] M. Lince-Faria, S. Maffini, B. Orr, Y. Ding, F. Cláudia, C.E. Sunkel, A. Tavares, J. Johansen, K.M. Johansen, H. Maiato, Spatiotemporal control of mitosis by the conserved spindle matrix protein Megator, J. Cell Biol. 184 (5) (2009) 647–657, https://doi.org/10.1083/jcb.200811012.

[35] M. Capizzi, R. Carpentier, E. Denarier, A. Adrait, R. Kassem, M. Mapelli, Y. Couté, S. Humbert, Developmental defects in Huntington's disease show that axonal growth and microtubule reorganization require NUMA1, Neuron 110 (1) (2022) 36–50.e35, https://doi.org/10.1016/j.neuron.2021.10.033.

[36] C. Ernst, Proliferation and differentiation deficits are a major convergence point for neurodevelopmental disorders, Trends Neurosci. 39 (5) (2016) 290–299, https://doi.org/10.1016/j.tins.2016.03.001.

[37] B.D. Freibaum, Y. Lu, R. Lopez-Gonzalez, N.C. Kim, S. Almeida, K.H. Lee, N. Badders, M. Valentine, B.L. Miller, P.C. Wong, L. Petrucelli, H.J. Kim, F.B. Gao, J. P. Taylor, GGGGCC repeat expansion in C9orf72 compromises nucleocytoplasmic transport, Nature 525 (7567) (2015) 129–133, https://doi.org/10.1038/nature14974.

[38] K. Zhang, C.J. Donnelly, A.R. Haeusler, J.C. Grima, J.B. Machamer, P. Steinwald, E.L. Daley, S.J. Miller, K.M. Cunningham, S. Vidensky, S. Gupta, M.A. Thomas, I. Hong, S.L. Chiu, R.L. Huganir, L.W. Ostrow, M.J. Matunis, J. Wang, R. Sattler, T.E. Lloyd, J.D. Rothstein, The C9orf72 repeat expansion disrupts nucleocytoplasmic transport, Nature 525 (7567) (2015) 56–61, https://doi.org/10.1038/nature14973.

[39] C.C. Chou, Y. Zhang, M.E. Umoh, S.W. Vaughan, I. Lorenzini, F. Liu, M. Sayegh, P.G. Donlin-Asp, Y.H. Chen, D.M. Duong, N.T. Seyfried, M.A. Powers, T. Kukar, C.M. Hales, M. Gearing, N.J. Cairns, K.B. Boylan, D.W. Dickson, R. Rademakers, Y.J. Zhang, L. Petrucelli, R. Sattler, D.C. Zarnescu, J.D. Glass, W. Rossoll, TDP-43 pathology disrupts nuclear pore complexes and nucleocytoplasmic transport in ALS/FTD, Nat. Neurosci. 21 (2) (2018) 228–239, https://doi.org/10.1038/s41593-017-0047-3.

[40] K.M. Cunningham, K. Maulding, K. Ruan, M. Senturk, J.C. Grima, H. Sung, Z. Zuo, H. Song, J. Gao, S. Dubey, J.D. Rothstein, K. Zhang, H.J. Bellen, T.E. Lloyd, TFEB/Mitf links impaired nuclear import to autophagolysosomal dysfunction in C9-ALS, Elife 9 (2020), https://doi.org/10.7554/eLife.59419.

[41] S.K. Dubey, K. Maulding, H. Sung, T.E. Lloyd, Nucleoporins are degraded via upregulation of ESCRT-III/Vps4 complex in Drosophila models of C9-ALS/FTD, Cell Rep. 40 (12) (2022) 111379, https://doi.org/10.1016/j.celrep.2022.111379.

[42] F. Gasset-Rosa, C. Chillon-Marinas, A. Goginashvili, R.S. Atwal, J.W. Artates, R. Tabet, V.C. Wheeler, A.G. Bang, D.W. Cleveland, C. Lagier-Tourenne, Polyglutamine-expanded huntingtin exacerbates age-related disruption of nuclear integrity and nucleocytoplasmic transport, Neuron 94 (1) (2017) 48–57.e44, https://doi.org/10.1016/j.neuron.2017.03.027.

[43] A.E. Molero, S. Gokhan, S. Gonzalez, J.L. Feig, L.C. Alexandre, M.F. Mehler, Impairment of developmental stem cell-mediated striatal neurogenesis and pluripotency genes in a knock-in model of Huntington's disease, Proc. Natl. Acad. Sci. U. S. A. 106 (51) (2009) 21900–21905, https://doi.org/10.1073/pnas.0912171106.

[44] S.K. Dubey, M.G. Tapadia, Yorkie regulates neurodegeneration through canonical pathway and innate immune response, Mol. Neurobiol. 55 (2) (2018) 1193–1207, https://doi.org/10.1007/s12035-017-0388-7.

[45] G.P. Ritson, S.K. Custer, B.D. Freibaum, J.B. Guinto, D. Geffel, J. Moore, W. Tang, M.J. Winton, M. Neumann, J.Q. Trojanowski, V.M. Lee, M.S. Forman, J. P. Taylor, TDP-43 mediates degeneration in a novel Drosophila model of disease caused by mutations in VCP/p97, J. Neurosci. 30 (22) (2010) 7729–7739, https://doi.org/10.1523/jneurosci.5894-09.2010.

[46] H. Lee, J.J. Lee, N.Y. Park, S.K. Dubey, T. Kim, K. Ruan, S.B. Lim, S.H. Park, S. Ha, I. Kovlyagina, K.T. Kim, S. Kim, Y. Oh, H. Kim, S.U. Kang, M.R. Song, T. E. Lloyd, N.J. Maragakis, Y.B. Hong, H. Eoh, G. Lee, Multi-omic analysis of selectively vulnerable motor neuron subtypes implicates altered lipid metabolism in ALS, Nat. Neurosci. 24 (12) (2021) 1673–1685, https://doi.org/10.1038/s41593-021-00944-z.

[47] F. Guo, M. Holla, M.M. Díaz, M. Rosbash, A circadian output circuit controls sleep-wake arousal in Drosophila, Neuron 100 (3) (2018) 624, https://doi.org/10.1016/j.neuron.2018.09.002, 635.e624.